RSC Advances

PAPER

View Article Online
View Journal | View Issue



Cite this: *RSC Adv.*, 2022, **12**, 28867

# Preparation and sustained-release properties of poly(lactic acid)/graphene oxide porous biomimetic composite scaffolds loaded with salvianolic acid B

Shuqiong Liu,[a] Zhenyi Xu,[a] Jiapeng Hu,[a] Zhenzeng Wu[a] and Yuying Zheng *[b]

Biomimetic scaffolds loaded with drugs can improve the osteogenesis and neovascularisation of scaffolds. A series of PLA/GO/Sal-B drug-loaded scaffolds was prepared by thermally induced phase separation. The addition of Sal-B increased the diameter of the fibres, but the scaffold showed a porous nanofibrous structure after drug release. X-ray diffraction results showed that the addition of Sal-B did not affect the formation of the nanofibre biomimetic structure of the scaffold. FTIR results indicated a certain interaction between Sal-B and PLA/GO. Water absorption and porosity test results revealed that the scaffolds had good hydrophilicity and appropriate porosity. The addition of Sal-B was also conducive to the formation of sediments possibly due to the good water solubility of Sal-B itself. The prepared scaffolds had good blood compatibility and cytocompatibility, and a small additional amount of Sal-B could significantly promote cell proliferation and alkaline phosphatase activity. Their sustained release performance indicated that the biomimetic scaffolds had controlled the release of Sal-B. The kinetic model showed that the PLA/GO/Sal-B drug-loaded biomimetic scaffolds followed the diffusion mechanism.

Received 27th August 2022
Accepted 1st October 2022

DOI: 10.1039/d2ra05371c

rsc.li/rsc-advances



## 1. Introduction

Bone tissue engineering materials for the repair of bone defects caused by accidents, sports injuries, tumours and osteoporosis are developing rapidly. The key to functional tissue-engineered bone regeneration is to develop biomimetic scaffolds with good cell migration, differentiation and functional expression.[1–3] The structural characteristics of scaffolds can affect metabolism, nutrient diffusion and neovascularisation, regulating cell response and improving tissue growth efficiency.[1,4] Functional bone regeneration scaffolds should meet certain standards in biocompatibility, bone conductivity, bone induction rate, mechanical properties and microstructure.[5,6] However, a structure of scaffold has limited effectiveness in regulating bone regeneration. Loading bioactive factors and drugs into multiple scaffolds could induce cell adhesion, proliferation and differentiation and enhance the effectiveness of integration with the surrounding tissues, improving the osteogenesis and neovascularisation of scaffolds.[7,8] Therefore, scaffolds combined with bioactive factors and drugs are preferred for bone repair and transplantation due to their exceptional bone inductivity. Osteoinduction is exhibited by many kinds of growth factors, among which BMP-2 has the most significant osteogenic effect.[9–14] Although the osteogenic effect can be improved by bone induction factors, their application is limited due to their disadvantages, such as high price, short half-life, high technical requirements for loading, easy inactivation and repeated use.[15] Additionally, osteogenesis is influenced by angiogenesis.[16] Bone tissue repair is a complicate physiological process. Take bone healing as an example, it includes local bleeding, inflammation, complex activities of mesenchymal precursor cells, and the gradual formation of soft extracellular matrix tissue, cartilage and new bone.[17,18] This process makes up of a coordinated series of cellular activities, including proliferation and differentiation of bone progenitor cells, tissue vascularization and bone tissue formation. Traditional Chinese medicine believes that fractures will experience redness and pain in the fracture area, swelling and poor circulation, slow bone healing and other symptoms. Therefore, eliminating inflammation, promoting blood circulation and stimulating bone regeneration are some strategies to improve bone healing.[18] Alternative osteogenic and angiogenic drugs with improved osteogenic effects must be urgently developed. Many studies focused on the development of osteogenic active drugs with low biotoxicity, such as bioactive molecules from traditional Chinese medicine.[19,20] The treatment of orthopaedic diseases with traditional Chinese medicine has been increasingly investigated, and the effects are

[a]College of Ecology and Resource Engineering, Wuyi University, Wuyishan 354300, People's Republic of China

[b]College of Materials Science and Engineering, Fuzhou University, Fuzhou, 350108, People's Republic of China. E-mail: yyzheng@fzu.edu.cn; Tel: +86-591-22866524

apparent. Many pharmacological and biological research shows that: a lot of Chinese herbal medicine is to maintain or improve the effect of bone health, including rhizoma drynariae, safflower, *Eucommia* bark, Fructus Ligustri Lucidi, yin grandiflorum, fructus sophorae, *Astragalus*, desertliving cistanche, *Cordyceps sinensis*, *Salvia miltiorrhiza*, *etc.*, but only yin grandiflorum have clinical research in the herb.[21]

Salvianolic acid B (Sal-B) is a famous traditional Chinese herbal medicine and a water-soluble phenolic acid extracted from the dried root or rhizome of *Salvia miltiorrhiza*, widely used in the treatment of angina pectoris, myocardial infarction, stroke and other cardiovascular diseases.[22,23] This compound has good cardiovascular regulatory effects, including improving heart function after ischaemia–reperfusion injury and myocardial infarction. Sal-B can also promote cell proliferation and differentiation, anti-apoptosis and anti-oxidation and maintain normal cell functions to reduce blood viscosity, infarction area, myocardial collagen volume and hypertrophy.[24,25] In addition to its good effects on cardiovascular diseases, Sal-B exhibits angiogenic and osteogenic activities.[16] Yan *et al.* showed that *S. miltiorrhiza* activates blood circulation, removes stasis, channels meridians, activates collaterals and has certain effects on different bone cells to stimulate osteogenesis and promote bone healing.[26] Cui *et al.* reported that *S. miltiorrhiza* extract has a positive influence on osteoporosis in rats mainly by promoting the secretion of osteocalcin and alkaline phosphatase (ALP); it also inhibits adipocyte formation and promotes osteoblast differentiation.[27] He *et al.* stated that Sal-B can accelerate early fracture healing and can be used as a treatment option for patients with traumatic fractures.[28] Huan *et al.* indicated that it is effective in orthopaedic repair and could improve the growth and mineralisation of osteoblasts.[29] Additionally, this compound can inhibit bone loss, promote vascularisation, stimulate cell metabolism, enhance cell differentiation and proliferation and thus accelerate bone healing.[21,30,31] It can also stimulate the total metabolic activity and ALP activity of osteoblasts through the ERK signalling pathway.[32] Therefore, Sal-B shows potential in inducing bone regeneration for bone tissue engineering in clinical application. However, limited reports are available on Sal-B-loaded porous biomimetic composite scaffolds with satisfying release behaviour and good bioactivity. Therefore, we tried to construct a drug-loaded scaffold with the controlled release of Sal-B to utilise the osteogenic and angiogenic bioactivities of this compound.

Drug-controlled release refers to the combination of drugs and carriers in a certain way (chemical or physical), and then, by means of penetration or diffusion, the drug is released in a fixed, sustained and stable manner at an appropriate concentration to achieve the purpose of drug therapy.[33–35] Meanwhile, drug carrier material is an important part of drug-controlled release, which plays a role in regulating drug release rate and influencing drug effect. Polylactic acid (PLA), a biocompatible, biodegradable and non-toxic polyester synthesized from renewable resources, has been studied for many years. PLA has been widely studied in biomedical applications such as drug delivery, sutures, implants and tissue engineering due to its adjustable degradation rate, excellent processing characteristics, unique pharmacokinetic and pharmacological efficacy.[36–38] Graphene oxide (GO) is a graphene derivative that has attracted much attention recently. The molecular structure of GO contains functional groups such as carboxyl, hydroxyl, carbonyl and epoxy groups, so it has strong activity and good hydrophilicity.[39] Meanwhile, there are some unoxidized aromatic regions on the basal surface of GO, which makes GO have certain hydrophobicity. Active functional groups on the surface of GO make it easy for GO to react with various polymers or drugs, forming chemical bonds or interactions (including hydrogen bonds, hydrophobic interactions, $\pi$–$\pi$ conjugation, *etc.*), so as to enhance the strength of the blend or improve the interaction between the carrier and drugs.

With previously prepared PLA/GO biomimetic scaffolds as the basis, Sal-B was introduced into scaffolds to prepare biomimetic scaffolds loaded with Sal-B with good sustained release and could play a certain role in bone repair. The structural morphology, chemical properties, water absorption and porosity of PLA/GO/Sal-B porous biomimetic composite scaffolds with different Sal-B contents were discussed, and their mineralisation performance, blood compatibility, cytotoxicity, ALP activity and sustained-release performance were evaluated. The mechanism of the sustained release of the drug-loaded scaffolds was also explained.

## 2. Materials and methods

### 2.1 Materials

PLA (3052D; $M_n$, 250 000 g mol$^{-1}$) was purchased from NatureWorks (USA), aspirin (ASA, AR.) was supplied by Aladdin Reagent Co., Ltd. (Shanghai, China) and Sal-B was acquired from Jiangsu Yongjian Pharmaceutical Technology Co., Ltd. (China). GO was prepared in our laboratory as described previously.[40] All other reagents and solvents used in this work were of analytical reagent grade and purchased from Sinopharm Chemical Reagent Co., Ltd. (China).

### 2.2 Fabrication of Sal-B-loaded porous biomimetic composite scaffolds

A specific amount of GO (fixed at 2.0 wt%, relative to PLA) was ultrasonically dispersed in dioxane/water for 30 min. The solution was successively added with PLA (10.0 wt%; w/w) and stirred at 60 °C until PLA was completely dissolved to obtain a homogeneous mixed solution. Different amounts of Sal-B were then successively added, and the mixture was stirred under dark for another 20 min to produce a series of homogeneous solution with different Sal-B contents (0, 1.0, 3.0 and 5.0 wt%, relative to PLA). The homogeneous solution was poured into a mould, aged at 0 °C overnight while being sheltered from the light until gel formation and finally frozen at −40 °C for 3 h. Finally, the scaffold was freeze-dried in vacuum (−54 °C) for 3 days and stored in a dry place away from light. Scaffolds prepared with 0, 1.0, 3.0 and 5.0 wt% Sal-B were designated Sal-B0, Sal-B1, Sal-B3 and Sal-B5, respectively.

### 2.3 Characterisation of PLA/GO/Sal-B drug-loaded porous biomimetic composite scaffolds

The morphology of PLA/GO/Sal-B drug-loaded porous biomimetic composite scaffolds with different Sal-B contents was observed by scanning electron microscopy (SEM) (Vega 3 SBH, TESCAN CO., Ltd.) before and after drug release and platelet adhesion. The influence of different Sal-B contents on the overall crystallinity of the drug-loaded biomimetic composite scaffold was analysed by X-ray diffraction (XRD) (D8 Advance, Bruker Ltd.). The functional groups of the PLA/GO/Sal-B biomimetic composite scaffold were characterised by Fourier transform infrared spectroscopy (FTIR, Nicolet IS5, Thermo fisher Ltd.) in transmission mode over the wavenumber range of 400–4000 $cm^{-1}$.

### 2.4 Water absorption and porosity

The porosity and water absorption of the PLA/GO/Sal-B drug-loaded porous biomimetic composite scaffolds were determined by referring to literature.[40,41]

### 2.5 Apatite-formation ability

The bioactivity of the PLA/GO/Sal-B composite scaffolds was measured in terms of their apatite-formation ability by immersing them in 1.5 SBF. Details of the apatite-formation ability test were described in a previous work.[41,42]

### 2.6 Cell culture

The biocompatibility of the drug-loaded porous biomimetic composite scaffolds was studied using a mouse pre-osteoblast cell line, MC3T3-E1 (Saibai Kang Biology, Shanghai, China). The cells were propagated in a conventional growth medium[43] and incubated in a humidified atmosphere of 5% $CO_2$ at 37 °C. The medium was replaced with a fresh one every 3 days.

### 2.7 Cell proliferation

The samples were cut into small pieces ($1 \times 10 \times 2$ $mm^3$) and UV disinfected for 24 h. The MC3T3-E1 cells were seeded in 24-well plates ($n = 3$) at a seeding density of $10^4$ cells per well, cultured with drug-loaded porous biomimetic composite scaffolds containing different Sal-B contents and incubated in a standard incubator (37 °C and 5% $CO_2$). Cell proliferation was investigated using Cell Counting Kit-8 (CCK-8, HY-K0301, MCE, USA). After the cells were cultured for 1, 3 and 5 days, the cell-seeded scaffolds were rinsed with phosphate-buffered saline (PBS) twice and incubated with 500 μL of CCK-8 solution (10%) for another 2 h at 37 °C and 5% $CO_2$. The formazan solution was transferred to a 96-well plate after incubation, and the optical density (OD) was measured at 450 nm using a microplate reader (EPOCH2, Biotek, USA). The obtained value was proportional to the number of adhered cells in each well.

### 2.8 Alkaline phosphatase activity

The osteogenic differentiation of MC3T3-E1 cells was evaluated by measuring their ALP activity. MC3T3-E1 cells were inoculated in six-well plates at a density of $1.0 \times 10^4$ cells per well and cultured adherent in a 5% $CO_2$, 37 °C constant temperature incubator. The scaffold with different Sal-B contents was then added into each group. The cells were collected at 3, 7 and 14 days, and the ALP expression was detected following the instructions of the ALP activity detection kit. For cell lysate preparation, the culture medium was removed. The cells were washed with PBS, digested with trypsin and added with 200 μL of protein lysate. The lysate was fully blown and centrifuged at 4 °C, 10 000×$g$ for 10 min. The supernatant was obtained for detection. Afterward, 50 μL of the sample was added to the well of the ELISA plate which was then vibrated for 30 s and incubated at 37 °C for 30 min. The reaction was stopped by adding 100 μL of stop solution to the well. The sample was thoroughly mixed, and the OD value was measured at 405 nm using a microplate tester.

### 2.9 *In vitro* release of Sal-B

The standard solutions of Sal-B were configured, and the absorbance of Sal-B standard solutions at 286 nm was measured using a UV-visible spectrophotometer (UV-1100, Shanghai Meipuda Instruments Co., Ltd.). Corresponding standard curves were also drawn. The release of Sal-B from the PLA/GO/Sal-B composite scaffold was measured by immersing a pre-weighed scaffold (approximately 0.03 g) in 25 mL of PBS (pH, 7.35) under constant temperature and stirring (150 rpm and 37 °C). An aliquot (3 mL) of the solution from the release medium was removed at pre-determined time points and replaced with fresh buffer (3 mL). The absorbance of Sal-B in the soak solution was measured at 286 nm, and the cumulative release percentage ($\eta$) was calculated as follows:

$$\eta = m_n \times 100\%/M$$

where $m_n$ is the amount of Sal-B released from the PLA/GO/Sal-B composite scaffold at time $t$, and $M$ is the total mass of Sal-B pre-loaded on the PLA/GO/Sal-B composite scaffold.

### 2.10 Haemocompatibility

The haemocompatibility of the PLA/GO/Sal-B drug-loaded biomimetic composite scaffold was measured using the haemolysis ratio and platelet adhesion rate. The experiment was conducted in strict accordance with the "Rules for the Ethical Review of Life Sciences and Medical Research Involving Humans", following the general procedures as employed at a different laboratory. The process used to collect and handle human whole blood was approved by the Institutional Review Board (IRB) at Fuzhou First Hospital. Informed consents were obtained from human participants of this study. Venous blood was collected from a healthy volunteer in trisodium citrate (9%) vials in accordance with ISO 10993-4:2017.[44] The haemolysis ratio was evaluated by measuring the relative amounts of haemoglobin released into the solution phase from the erythrocytes in whole blood exposed to the test materials.[45]

Small pieces ($1\ cm^2 \times 0.1$ cm) of PLA/GO/Sal-B drug-loaded porous biomimetic composite scaffolds were placed in tubes

with 10 mL of normal saline and kept warm at 37 °C for 30 min. For haemolytic rate quantification, 0.2 mL of diluted anticoagulant blood (8 mL of fresh anticoagulant blood in 10 mL 0.9% normal saline) was added into the tubes to soak the composite scaffold at 37 °C for 60 min under gentle agitation. Additionally, 0.2 mL of diluted anticoagulant blood was added to tubes with normal saline and distilled water to serve as negative and positive controls, respectively. The control group was also subjected to constant temperature oscillation at 37 °C for 60 min. After the pre-determined culture time was completed, the immersion solution was centrifuged at 2000 rpm for 10 min, and the absorbance of the supernatant was determined at 540 nm *via* spectrophotometry. The final data from each group were obtained by averaging the values of three samples. The haemolytic rate was calculated using the following formula:[46]

$$\mathrm{HR}\ (\%) = \frac{X_{\mathrm{ts}} - X_{\mathrm{nc}}}{X_{\mathrm{pc}} - X_{\mathrm{nc}}} \times 100\%$$

where $X_{\mathrm{ts}}$ is the absorbency of the test scaffold, and $X_{\mathrm{nc}}$ and $X_{\mathrm{pc}}$ are the absorbance values of negative and positive controls, respectively.

The PLA/GO/Sal-B drug-loaded composite scaffolds (1 $\mathrm{cm}^2$ × 0.05 cm) were immersed in normal saline and incubated at 37 °C for 2 h to investigate their platelet adhesion. Fresh human anticoagulant blood was centrifuged at 3000 rpm for 20 min to obtain platelet-rich plasma (PRP). Normal saline was removed, and 0.2 mL of fresh PRP was added on the surface of the PLA/GO/Sal-B drug-loaded porous biomimetic composite scaffolds which were maintained at 37 °C for 2 h. The scaffolds were then carefully rinsed with normal saline three times to remove the non-adherent platelets. Finally, the scaffolds were fixed to the platelets using 2.5 wt% glutaraldehyde at 4 °C for 1 h. The samples were rinsed with PBS twice and dehydrated by immersing them into a series of ethanol–deionised water solutions (50%, 60%, 80%, 90% and 100% [v/v]) for 30 min each. After dehydration, the samples were incubated at 4 °C for 24 h and vacuum freeze-dried for further use. Platelet adhesion was observed under SEM after gold coating.

### 2.11 Statistical analysis

All *in vitro* experiments were performed in triplicate, and data were expressed as means ± standard deviation (SD). Statistical analysis was conducted using GraphPad Prism software (v. 7.0). *P*-values between two groups were determined using Student's *t*-test. $P < 0.0001$ was considered statistically significant.

## 3. Results and discussion

### 3.1 Morphology of PLA/GO/Sal-B drug-loaded porous biomimetic composite scaffolds

Fig. 1 shows the morphological evolution of the sections of PLA/GO/Sal-B porous biomimetic composite scaffolds with different Sal-B contents. In this image, the whole and internal structure of the scaffolds can be observed. Fig. 1a1–d1 display that the morphology of the scaffold changed greatly with the addition of Sal-B. The size of spherulite particles and holes in the spherulite also increased significantly, forming the scaffold with a large pore structure (~100 μm level). However, the change of Sal-B content had minimal influence on the scaffold morphology, which maintained a consistent 3D porous structure. Fine powdery and sporadic flake structures were found on the surface of the scaffold and can be attributed to the precipitation of GO.[40] Meanwhile, Sal-B was evenly distributed in the scaffold. The enlarged morphology of the porous scaffold (Fig. 1b2–d2) revealed that the skeleton of the scaffold was composed of a micron fibre network. Compared with those in the PLA/GO scaffold (Fig. 1a2), the fibre diameter was larger, and the GO film on the surface became thicker and fitted the skeleton in the PLA/GO/Sal-B biomimetic composite scaffold. These results indicated that the addition of Sal-B did not change the biomimetic micro-nano fibre structure of the scaffold but promoted the growth of PLA spherulites and increased the fibre diameter.

### 3.2 XRD and FTIR of PLA/GO/Sal-B drug-loaded porous biomimetic composite scaffolds

Fig. 2 shows the XRD patterns of pure Sal-B and PLA/GO/Sal-B drug-loaded biomimetic nanofibrous composite scaffolds. An insignificant peak package of Sal-B appeared at about 20°, indicating that Sal-B is an amorphous or weakly crystalline

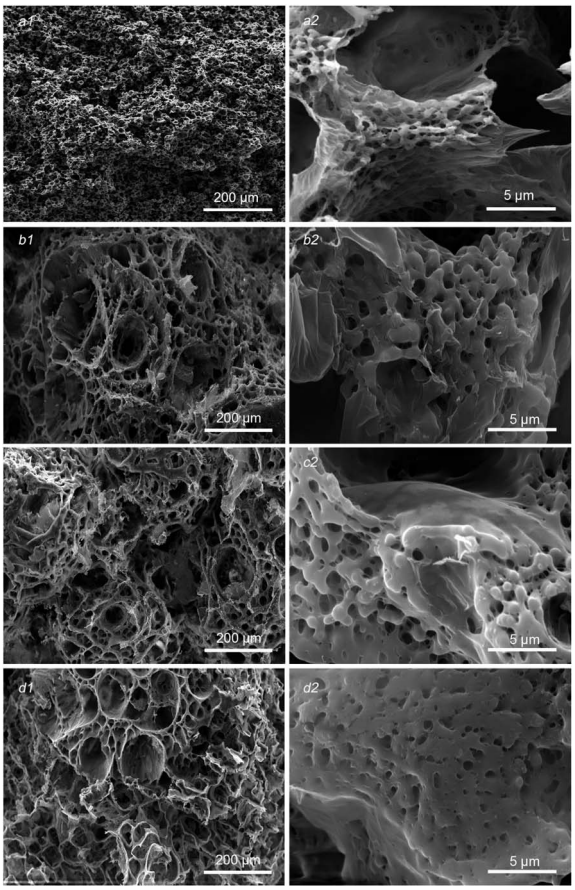


Fig. 1 Morphology of PLA/GO/Sal-B drug-loaded porous biomimetic composite scaffolds with different Sal-B contents: (a1 and a2) 0 wt%, (b1 and b2) 1 wt%, (c1 and c2) 3 wt%, (d1 and d2) 5 wt%.

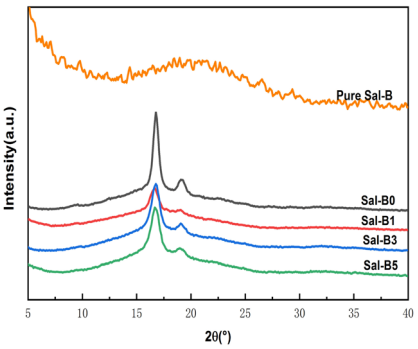


Fig. 2 XRD of pure Sal-B and PLA/GO/Sal-B drug-loaded porous biomimetic nanofibrous scaffolds with different Sal-B contents.

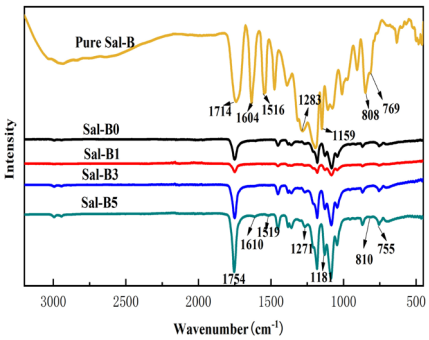


Fig. 3 FTIR of pure Sal-B and PLA/GO/Sal-B drug-loaded porous biomimetic composite scaffolds with different Sal-B contents.

material. The characteristic diffraction peaks of PLA at 17° and 19° could be seen in the XRD patterns of composite scaffolds with different Sal-B contents,[47] but the peak intensity changed greatly with the addition of Sal-B. The addition of 1 wt% Sal-B significantly reduced the intensity of the characteristic diffraction peak of PLA at 17°, and only one bulge of the diffraction peak remained at 19°. Similarly, the diffraction peak of PLA composite scaffold with the addition of 3 and 5 wt% Sal-B was also weakened but remained stronger than that of PLA with the addition of 1 wt% Sal-B. These results showed that the addition of a small amount of Sal-B had a great effect on the crystal structure of PLA, and this influence decreased when the Sal-B content was increased to 3 and 5 wt%. This phenomenon can be explained as follows: a small amount of Sal-B can be evenly dispersed in the system and be compatible with PLA at the molecular level, affecting the formation of PLA spherulites and resulting in the imperfect growth of spherulites and reduced crystallinity. However, Sal-B agglomerates when its addition amount increases. As a result, the microscopic size of Sal-B in the system increases, affecting the compatibility of PLA and Sal-B. Therefore, the interference of Sal-B on the generation of PLA spherulites is reduced during the crystallisation of PLA, and the crystallinity of the material increases. Therefore, the peak intensity increases. XRD results showed that although the addition of Sal-B changed the overall crystallisation performance of the scaffold, it did not affect the generation of PLA spherulite. Therefore, the addition of Sal-B will not affect the formation of the biomimetic porous nanofibrous structure of the scaffold.

Fig. 3 shows the FTIR diagram of pure Sal-B and PLA/GO/Sal-B drug-loaded porous biomimetic composite scaffolds with different Sal-B contents. The characteristic absorption bands of pure Sal-B were located at 1604 and 1516 $cm^{-1}$ (aromatic compound skeleton vibration), 1283 and 1159 $cm^{-1}$ (C–O stretching) and 808 and 769 $cm^{-1}$ (O–H bending);[1] among which 1604 $cm^{-1}$ is the stretching vibration of C=O, implying the characteristic absorption of phenolic acid.[48] The characteristic absorption peaks of PLA[40] at 1747, 1184, 1084, and 869 $cm^{-1}$ were observed in all curves of PLA/GO/Sal-B composite scaffolds with different Sal-B contents. However, the peak intensity decreased firstly and then increased with the increase in Sal-B content. This finding was similar to the XRD results and may be caused by the dispersion of Sal-B in the composite system. Sal-B at 1 wt% is evenly dispersed, thus shielding the characteristic groups of PLA and reducing the detection sensitivity. However, when the content of Sal-B increases, its particles aggregate to some extent, thus reducing the shielding effect and increasing the sensitivity response of the groups. Additionally, the characteristic absorption peaks of PLA with 3 and 5 wt% Sal-B composite scaffolds were stronger than those of PLA without Sal-B composite scaffolds possibly due to the existence of GO. GO and Sal-B contain many hydroxyl groups, and the two may form a certain intermolecular hydrogen bond that will play a certain role in the subsequent slow release of Sal-B. Meanwhile, the spectrogram showed that the characteristic absorption peak of Sal-B gradually increased with the Sal-B content. The relatively pure Sal-B showed a certain degree of red shift or blue shift, indicating a certain interaction between Sal-B and PLA/GO, which will play a certain role in the subsequent slow-release control of Sal-B.

### 3.3 Water absorption and porosity of PLA/GO/Sal-B drug-loaded porous biomimetic composite scaffolds

Scaffolds with high hydrophilicity are highly conducive to cell proliferation and functional expression.[49] As shown in Fig. 4a, the water absorption rate of PLA/Sal-B/GO composite scaffold increased gradually with the Sal-B content and had values of 98.84% ± 14.75%, 152.7% ± 8.50% and 234.9% ± 20.77%. Given that Sal-B is a water-soluble phenolic acid, the water absorption rate of the composite scaffold increased with the Sal-B content. But the properties and structure of drug-loaded matrix are also essential factors for the hydrophilicity of composite scaffolds. As showed in Fig. 1, PLA/GO/Sal-B drug-loaded composite scaffolds with different Sal-B content all had 3D porous structure, but the hole size was small. Therefore, connectivity of hydrophilic components on the surface of the scaffold became an important factor for the hydrophilicity. This study uses PLA/GO as the drug-loaded matrix, where the hydrophilicity and amphiphilicity of GO can effectively improve the hydrophilicity of PLA.[40] In particular, the amphiphilicity of GO not only enables GO to cover the PLA surface evenly, but also promotes the uniform dispersion of Sal-B in the drug-loaded

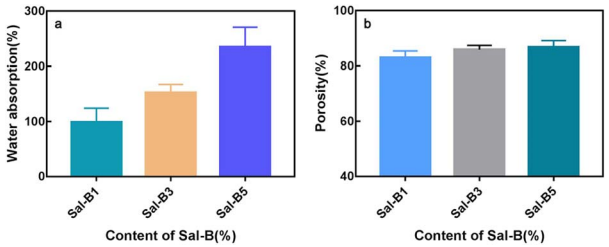


Fig. 4 Water absorption (a) and porosity (b) of PLA/GO/Sal-B drug-loaded porous biomimetic composite scaffolds with different Sal-B contents.

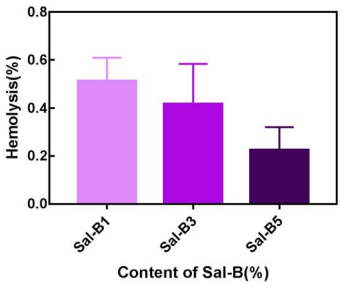


Fig. 6 Haemolysis rate of PLA/GO/Sal-B drug-loaded porous biomimetic composite scaffolds with different Sal-B contents.

matrix.[40] Therefore, with the increase of Sal-B content, the increase of water absorption is not only because Sal-B is a hydrophilic substance, but more importantly because with the increase of Sal-B content, the connectivity of Sal-B on the surface of the scaffold matrix is stronger, which is more conducive to the transport of water molecules in the whole scaffold. Therefore, the improvement of the water absorption of the scaffold is the comprehensive result of the structure and composition of the scaffold. On the one hand, the improvement of water absorption is beneficial to the transport of various mineral ions in body fluids and the application of scaffolds in tissue construction. On the other hand, it will facilitate the diffusion and dissolution of the drug in the solution.

Fig. 4b shows the porosity of PLA/GO/Sal-B drug-loaded porous biomimetic composite scaffolds with different Sal-B contents. High porosity is one of the conditions for the application of composite materials as bone tissue engineering scaffolds that guide bone tissue regeneration and promote the growth of new bones. An 80% porosity can meet the requirements of scaffolds.[50] Fig. 4b shows that the porosities of the composite scaffolds were 83.04% ± 2.38%, 85.85% ± 1.56% and 86.83% ± 2.34%, indicating that the porosity of the prepared composite scaffolds can meet the requirements for tissue engineering. SEM results (Fig. 1) also showed that the composite scaffolds with different Sal-B contents had similar pore structure and pore size distribution, and the pore size distribution was in different orders of magnitude, including nano and micron pores. These holes of different sizes are the reason why the porosity of the three scaffolds remains the same. They also provide the scaffolds with several functions, such as nutrient transport and cell migration.

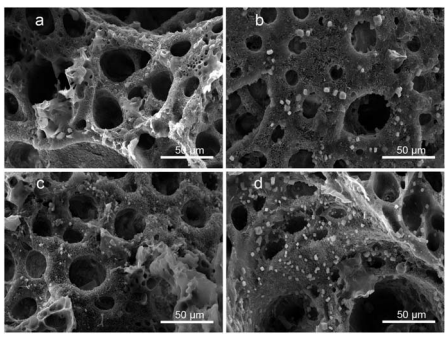


Fig. 5 Morphology of the PLA/GO/Sal-B drug-loaded biomimetic nanofibrous scaffold after being immersed in SBF for 3–14 days: 1 wt% 3 days (a), 7 days (b), 14 days (c) and 5 wt% 3 days (d).

### 3.4 Apatite-formation ability of PLA/GO/Sal-B drug-loaded porous biomimetic composite scaffolds

Fig. 5 shows the morphology of the PLA/GO/Sal-B drug-loaded biomimetic nanofibrous scaffold after being immersed in SBF for 3–14 days. The results showed that all the scaffolds formed square sediments on their surface after being soaked in SBF. These square deposits are hydroxyapatite.[42] Comparison of Fig. 5a–c revealed that the number of particles formed on the surface of the scaffold increased with the soaking days, indicating that the ability of the scaffold maintained its ability to induce sediment formation over time. Compared with the addition of 1 wt% Sal-B, the addition of 5 wt% Sal-B led to greater sediment deposition on the surface of the scaffold soaked SBF for 3 days, indicating that the addition of Sal-B in the composite scaffold is conducive to the formation of sediment. This finding can be attributed to the good water solubility of Sal-B. Water absorption analysis revealed that the water absorption of composite scaffold increased with the Sal-B content. The scaffold-induced apatite formation is the diffusion of $Ca^{2+}$, $PO_4^{3-}$ and $OH^-$ from the SBF-saturated solution to the surface of the scaffold and the formation of sediment.[42] Therefore, the diffusion of ions must affect the formation rate and amount of sediment. Good hydrophilicity is conducive to the diffusion of ions to the surface of the scaffold in the solution and consequently to the bio-mineralisation of the scaffold.

### 3.5 Haemocompatibility of PLA/GO/Sal-B drug-loaded porous biomimetic composite scaffolds

The haemolysis rate represents the degree of haemolysis when red blood cells come in contact with the scaffold material. In addition to the cytocompatibility of scaffolds, haemocompatibility is also an important evaluation aspect for their application as bone tissue engineering materials. As shown in Fig. 6, the haemolysis rates of different Sal-B drug-loaded porous biomimetic composite scaffolds were all <1 wt%. Therefore, all the prepared PLA/GO/Sal-B drug-loaded porous biomimetic composite scaffolds are non-haemolysis materials following ASTM F756-00 (2000) standard. This result was consistent with

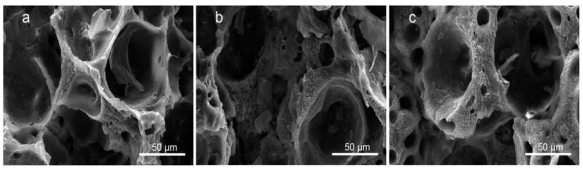


Fig. 7 SEM of platelet adhesion for PLA/GO/Sal-B drug-loaded porous biomimetic composite scaffolds with different Sal-B contents: (a) 1 wt%, (b) 3 wt% and (c) 5 wt%.

the haemolysis of other Sal-B composite scaffolds.[22,48] Additionally, the haemolysis rate of the composite scaffold showed a downward trend with the addition of Sal-B, indicating that the addition of Sal-B is beneficial to reduce the haemolysis rate. In conclusion, the PLA/GO/Sal-B drug-loaded porous biomimetic composite scaffolds with different Sal-B contents have good haemocompatibility and are suitable for scaffold transplantation in tissue engineering.

Fig. 7 shows the SEM images of composite scaffolds with different Sal-B contents (1, 3 and 5 wt%) after the platelet adhesion experiment. No platelet adhesion was observed on the surface of the scaffolds. The surface properties, hydrophilicity and composition of composite scaffolds influence their platelet adhesion,[51] but the addition of Sal-B played the main role in this experiment. Ren *et al.* reported that Sal-B plays an important role in the cardiovascular field because of its inhibitory effect on platelet adhesion and aggregation.[52,53] Liu *et al.* studied the antiplatelet effect of Sal-B and found that Sal-B had a good antiplatelet effect and suppressed human platelet activation by inhibiting PDE and antagonising P2Y12.[51] Therefore, the PLA/GO/Sal-B composite scaffolds have good blood compatibility.

### 3.6 Cell proliferation of PLA/GO/Sal-B drug-loaded porous biomimetic composite scaffolds

CCK-8 assays were used to investigate the proliferation of MC3T3-E1 cultured on PLA/GO/Sal-B porous biomimetic composite scaffolds with different Sal-B contents. Fig. 8 shows that all MC3T3-E1 cells could proliferate on the drug-loaded porous biomimetic composite scaffolds, and no statistical difference was observed among the groups after a 1-day culture. After 3 days of culture, the cell proliferation on Sal-B0, Sal-B1 and Sal-B3 scaffolds was significant ($P < 0.0001$). No difference was found between the Sal-B1 and Sal-B3 groups ($P > 0.05$), but the cell proliferation of the Sal-B5 group was inhibited. After 5 days of scaffold culture, the proliferation of the Sal-B0 and Sal-B1 groups was still significant, and that of the Sal-B1 group was significantly higher than that of the Sal-B0 group ($P < 0.0001$). Meanwhile, the cell proliferation of the Sal-B3 group was somewhat inhibited, and no significant difference in cell proliferation was observed for the Sal-B5 group on days 3 and 5. The results showed that a small amount of Sal-B (1%) was beneficial to the proliferation of MC3T3-E1 cells. The Sal-B3 group showed a certain inhibitory effect on the proliferation of MC3T3-E1 cells after 5 days of scaffold culture, and this influence may be related to the amount of Sal-B released in the scaffold. Therefore, Sal-B has no cytotoxicity and can promote

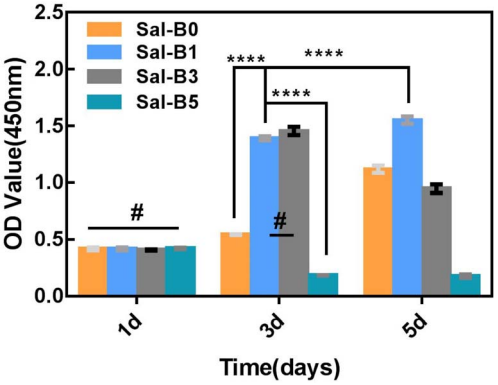


Fig. 8 MC3T3-E1 cell proliferation on PLA/GO/Sal-B drug-loaded porous biomimetic composite scaffolds with different Sal-B content after 1, 3 and 5 days of culture ($n = 3$, mean ± SD, #$P > 0.05$ and **** $P < 0.0001$).

cell proliferation within a certain dosage range. The effect of Sal-B on cells depends on cell type, dosage and loaded matrix. Shoba *et al.* reported that the cell viability of pure salvianolic acid B was about 80% after 48 h of culture, showing low cytotoxicity. However, if combined with bromelain loaded on PCL/PVA: GE NF scaffold, the cell viability was better, higher than 90%. They believe that the biomimetic structure of nanofibers is one of the reasons for the compatibility of scaffolds.[48] Lin *et al.* also fabricated PLGA/β-TCP scaffolds incorporated with different doses of Sal-B, and the results indicated no dose dependent effect in cell viability rate.[25] Ji *et al.* also reported that the biocompatibility of the Sal B-CS/HA was favorable by evaluation of cell morphology and proliferation.[16] Although previous studies have shown that Sal-B has low toxicity to cells, only one salvianolic acid B content was generally considered in these studies, so the toxic effect of Sal-B content on scaffold remains to be supported by more researches. Some studies even believe that the biomimetic structure of scaffolds is a major reason for the biocompatibility of cells. We believe that the cytocompatibility of scaffolds is the result of synergistic effects of scaffold structure, composition and Sal-B dosage.

### 3.7 ALP activity of PLA/GO/Sal-B drug-loaded porous biomimetic composite scaffolds

ALP is an important specific marker of early osteogenic differentiation. MC3T3-E1 cells were inoculated on porous biomimetic composite scaffolds to evaluate the osteogenic differentiation effect of different Sal-B contents. The ALP activity of MC3T3-E1 cells was measured at 3, 7 and 14 days. Fig. 9 shows that the expression activity of ALP increased with time and was concentration-dependent. After 3 days of scaffold culture, the ALP activity in Sal-B1 and Sal-B3 groups was significantly higher than that in Sal-B0 and Sal-B5 groups ($P < 0.0001$). Meanwhile, the ALP activity in the Sal-B3 group was significantly higher than that in Sal-B1 ($P < 0.01$), and no difference was observed between Sal-B0 and Sal-B5 groups ($P > 0.05$). After 7 and 14 days of scaffold culture, the ALP activity in the Sal-B0 and Sal-B1 groups continued to increase significantly

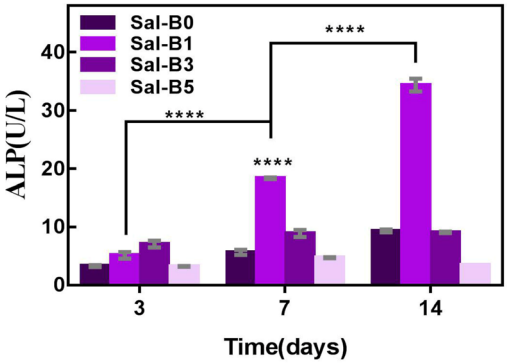


Fig. 9 ALP activity of MC3T3-E1 cells cultured with PLA/GO/Sal-B drug-loaded porous biomimetic composite scaffolds with Sal-B different contents for 3, 7 and 14 days ($n$ = 3, mean ± SD, ****$P$ < 0.0001).

($P$ < 0.0001). In the Sal-B3 group, ALP was significantly increased after 7 days of scaffold culture, but no significant difference was observed after 14 days ($P$ > 0.05). The ALP activity in the Sal-B5 group decreased after 14 days of culture, *i.e.* the expression and activity of ALP in the Sal-B3 group were the highest on the 3rd day of culture. However, in the subsequent experiments, the expression and activity of ALP in the Sal-B1 group were the highest, and the ALP activity of the Sal-B3 and Sal-B5 groups were inhibited to some extent. Therefore, the Sal-B1 group had the best effect of inducing osteogenic differentiation within the experimental range, and the addition of Sal-B was beneficial to the osteogenic differentiation of scaffolds. Sal-B is a bioactive plant molecule with properties of bone induction,[31,32] angiogenesis promotion[25] and low cytotoxicity.[48,54] Wu *et al.* showed that Sal-B could significantly promote the osteogenic differentiation of rBMSCs by ALP and alizarin red staining *in vitro*; however, no statistically significant difference was found between the medium-dose and high-dose groups in this experiment.[19] Ji *et al.* showed that compared with the CS/HA group, the ALP activity and vascular endothelial growth factor activity increased in the Sal-B/CS/HA group.[16] The presence of Sal-B can promote bone regeneration and blood vessel formation and has a good effect on the repair of the bone defect. Further studies are warranted to determine whether the incorporation of high or low concentrations of Sal-B enhances angiogenesis and osteogenesis. Lin *et al.* prepared PLGA/TCP loaded Sal-B composite scaffold and found that the loaded Sal-B was released stably from the scaffold and the released Sal-B promoted the bone formation and angiogenesis in a dose-dependent manner *in vitro*.[25]

### 3.8 Release behaviour of Sal-B from PLA/GO/Sal-B drug-loaded porous biomimetic composite scaffolds

**3.8.1 Structural morphology of Sal-B drug-loaded scaffolds after sustained release.** Fig. 10 is the SEM of PLA/GO/Sal-B porous biomimetic composite scaffolds with different Sal-B contents soaked in PBS buffer solution for 9 days. Compared with Fig. 1a2–c2, the image showed the uniform nanofibre network structure of the scaffold. The fibre diameter was smaller than that before the sustained release and changed from the original micron-level to nano-level. Nanofibre networks were visible. Although the fibre diameter of PLA/GO/Sal-B drug-loaded scaffolds was larger than 1000 nm before the sustained release, it decreased significantly after the sustained release. The surface of the fibre skeleton of the drug-loaded biomimetic scaffolds was covered with Sal-B. When the scaffolds were immersed in PBS, the water-soluble Sal-B on the surface dissolved and diffused into the solution and the fibre diameter was consequently and significantly reduced. The SEM diagram after sustained release showed that the PLA/GO/Sal-B drug-loaded porous biomimetic composite scaffolds still had the micro-nano fibre structure of their biomimetic extracellular matrix after the sustained release of Sal-B. This finding indicated the preserved advantages of the biomimetic structure, which plays an important role in subsequent scaffold-induced cell adhesion, proliferation and other functions.

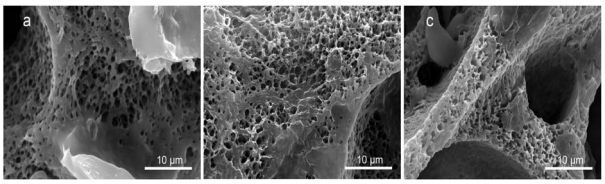


Fig. 10 Morphologies of PLA/GO/Sal-B drug-loaded porous biomimetic composite scaffolds with different Sal-B contents: (a) 1 wt%, (b) 3 wt% and (c) 5 wt%.

**3.8.2 Cumulative release of Sal-B drug-loaded scaffolds after sustained release.** As an ideal bone graft repair material, drug-loaded scaffolds should have good release performance, controlled drug release and maintain local drug concentration for a long time. The loading mechanism of Sal-B in the carrier is in an important influence on the sustained-release performance and kinetics of Sal-B. In this paper, Sal-B is directly added during the phase separation process of the scaffold, so it can be evenly dispersed on the surface and inside of the scaffold. The GO in drug scaffold is a great sustained-release drug carrier. Its

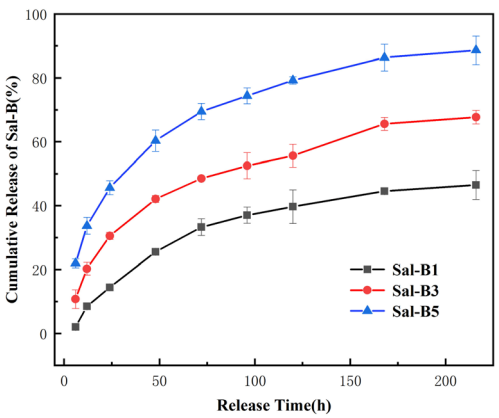


Fig. 11 Cumulative release of Sal-B from PLA/GO/Sal-B drug-loaded porous biomimetic composite scaffolds with different Sal-B contents.

Table 1 Fitting equation of drug release kinetics of Sal-B from PLA/GO/Sal-B drug-loaded porous biomimetic composite scaffolds with different contents of Sal-B

| Model | | | | |
|---|---|---|---|---|
| Sample | Zero-order | First-order | Higuchi | Hixson–Crowell |
| Sal-B1 | $Q_t = 0.204t + 10.642$ | $\ln(1 - Q_t) = -0.003t + 4.498$ | $Q_t = 3.752t^{1/2} - 3.172$ | $(1 - Q_t)^{1/3} = -0.004t + 4.475$ |
| Sal-B3 | $Q_t = 0.251t + 22.507$ | $\ln(1 - Q_t) = -0.005t + 4.373$ | $Q_t = 4.574t^{1/2} + 5.803$ | $(1 - Q_t)^{1/3} = -0.006t + 4.281$ |
| Sal-B5 | $Q_t = 0.295t + 37.222$ | $\ln(1 - Q_t) = -0.009t + 4.218$ | $Q_t = 5.446t^{1/2} + 17.018$ | $(1 - Q_t)^{1/3} = -0.009t + 4.022$ |

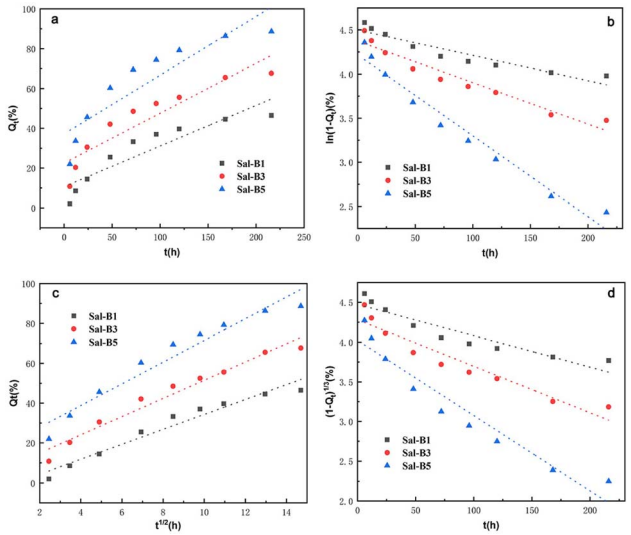


Fig. 12 Drug release kinetic model plots of Sal-B from PLA/GO/Sal-B drug-loaded porous biomimetic composite scaffolds with different Sal-B contents: zero-order (a), first-order (b), Hixson–Crowell (c) and Higuchi (d).

molecular structure contains a variety of active functional groups, and this compound easily forms π–π conjugation with drugs containing a benzene ring.[55] At the same time, the molecular structure of Sal-B contains a benzene ring and more hydroxyl groups. Therefore, GO enhances the interaction between drugs and the carrier and plays an important role in the sustained release of drugs. Depending on the result of FTIR, there are certain interactions between Sal-B and PLA/GO, including hydrogen bond between Sal-B and PLA, and π–π conjugate interaction between Sal-B and GO. These interactions will make Sal-B have excellent sustained-release performance. Fig. 11 displays the cumulative drug release curve of the PLA/GO/Sal-B drug-loaded biomimetic scaffolds soaked in PBS for 9 days. The result showed that the cumulative release of Sal-B gradually increased with the Sal-B content and had the values of 46.49%, 67.69% and 88.62% after 9 days. The three drug-loaded scaffolds with different Sal-B contents showed a similar cumulative release curve trend, *i.e.* before 72 h, they all had a fast release rate and a large cumulative release amount reaching 33.29%, 48.54% and 69.46%. However, from the 4th day of the experiment, the cumulative release rate and amount of the drug significantly slowed down and decreased, indicating that the scaffold could continuously release Sal-B. This release process may be related to the solubility of Sal-B and its distribution in the scaffold. The prepared drug-loaded scaffold is a nanofibre scaffold with a 3D porous structure. This nanofibre structure enables the scaffold to have a large specific surface area, so the distribution of Sal-B on the surface of the scaffold increases with the content of Sal-B. Meanwhile, Sal-B is a water-soluble small molecule. When the scaffold is immersed in PBS solution, the Sal-B on the surface of the nanofibre scaffold firstly dissolves and diffuses into the solution, and the PBS solution then penetrates the scaffold through the pores. Finally, the nanofibre-coated Sal-B is released due to the swelling or degradation of the nanofibres. The degradation rate of the matrix polylactic acid of this scaffold is slow and can be ignored during the experimental time. Therefore, the drug release mechanism of this series of drug-loaded scaffolds is mainly the diffusion of Sal-B. The diffusion of Sal-B is not only related to its properties but also the structure of the carrier and the interaction between the carrier and Sal-B. Wu *et al.* showed that different doses of Sal-B have similar release rates and could be continuously released from the scaffold.[19] The rough and porous structure is conducive to the adsorption of Sal-B. Especially, the dispersion of small pore size plays an important role in the extension of the release of Sal-B. The GO in drug scaffold is a good sustained-release drug carrier. Its molecular structure contains a variety of active functional groups, and this compound easily forms π–π conjugation with drugs containing a benzene ring.[55] Therefore, GO enhances the interaction between drugs and the carrier and plays an important role in the sustained release of drugs.

**3.8.3 Release kinetics model of Sal-B.** Zero-order, first-order, Higuchi and Hixson–Crowell models were used for the linear fitting of drug release behaviour to explore the drug release mechanism *in vitro* and clarify the drug release kinetics

Table 2 Fitting parameters of drug release kinetics Sal-B from PLA/GO/Sal-B drug-loaded biomimetic nanofibrous scaffolds with different contents of Sal-B

| Model | Zero-order | | First-order | | Higuchi | | Hixson–Crowell | |
|---|---|---|---|---|---|---|---|---|
| Parameter | | | | | | | | |
| Sample | $R^2$ | $k_0$ | $R^2$ | $k_1$ | $R^2$ | $k_H$ | $R^2$ | $k_{HC}$ |
| Sal-B1 | 0.8139 | 0.204 | 0.8701 | 0.003 | 0.9497 | 3.752 | 0.8521 | 0.004 |
| Sal-B3 | 0.8332 | 0.251 | 0.9286 | 0.005 | 0.9576 | 4.574 | 0.9009 | 0.006 |
| Sal-B5 | 0.7917 | 0.295 | 0.9590 | 0.009 | 0.9377 | 5.446 | 0.9142 | 0.009 |

of PLA/GO/Sal-B drug-loaded porous biomimetic composite scaffolds. The fitted equations and parameters are shown in Tables 1 and 2, and the fitting curves of the four models are displayed in Fig. 12. The Higuchi model had the largest correlation coefficient $R^2$ among the four models, indicating that the drug release mechanism of Sal-B in these composite scaffolds is mainly diffusion. As a small-molecule drug with a variety of biological activities, Sal-B easily diffuses from the scaffold skeleton, and its diffusion process is related to the performance, structure and porosity of the scaffold itself.[16]

## 4. Conclusions

A series of PLA/GO/Sal-B drug-loaded porous biomimetic composite scaffolds with different Sal-B contents was prepared by thermally induced phase separation. The addition of Sal-B increased the diameter of the fibres, but the scaffold showed a porous nanofibrous structure after drug release. XRD results showed that the addition of Sal-B did not affect the formation of the nanofibre biomimetic structure of the scaffold. FTIR results indicated a certain interaction between Sal-B and PLA/GO, which would play a certain role in the subsequent slow-release control of Sal-B. Test results for water absorption and porosity revealed that the scaffolds had good hydrophilicity and appropriate porosity. The addition of Sal-B was also conducive to the formation of sediments possibly due to the good water solubility of Sal-B itself. The test results of haemolysis ratio and platelet adhesion showed that the prepared scaffolds had good blood compatibility. Cell proliferation test results indicated that the scaffolds had cytocompatibility, and the addition of a small amount of Sal-B could significantly promote cell proliferation and ALP activity. The sustained release performance of the biomimetic scaffolds confirmed their ability for the controlled release of Sal-B. The kinetic model showed that the PLA/GO/Sal-B drug-loaded biomimetic scaffolds conformed to Higuchi's model, indicating that the drug release mechanism of Sal-B in this composite scaffold is mainly diffusion.

## Conflicts of interest

There are no conflicts to declare.

## Acknowledgements

This work was supported by Natural Science Foundation of Fujian Province of China (No. 2020J01416), Education and Scientific Research Project for Young and Middle-Aged Teachers in Fujian Province (No. JAT190765), The Financial support of this research from the Quanzhou Science and Technology Program of China (2021C002R), The Fujian Provincial Science and Technology Major Special Project (2021HZ027002), The Fujian Provincial Science and Technology Plan Project (2020H4010), Science and Technology Project of Nanping City (2022-ZXHZ-002, N2020Z015). The authors would like to thank the Hong Haifeng Research Group (Department of Orthopedics, Fuzhou First Hospital) for kindly providing haemocompatibility of scaffold.

## Notes and references

1 J. Li, Q. Wang, W. Zhi, J. Wang, B. Feng, S. Qu, Y. Mu and J. Weng, *Biomed. Mater.*, 2016, **11**, 055014.
2 V. Karageorgiou and D. Kaplan, *Biomaterials*, 2005, **26**, 5474–5491.
3 A. My, B. Ht, C. Bh, A. Ht, D. Rss, A. Et, A. Ak and C. Sg, *Biocybern. Biomed. Eng.*, 2020, **40**, 1626–1637.
4 F. P. Melchels, A. M. Barradas, C. A. Van Blitterswijk, J. De Boer, J. Feijen and D. W. Grijpma, *Acta Biomater.*, 2010, **6**, 4208–4217.
5 J. M. Holzwarth and P. X. Ma, *Biomaterials*, 2011, **32**, 9622–9629.
6 F. Du, H. Wang, W. Zhao, D. Li, D. Kong, J. Yang and Y. Zhang, *Biomaterials*, 2012, **33**, 762–770.
7 J. M. Kim, T. S. Han, M. H. Kim, D. S. Oh, S. S. Kang, G. Kim, T.-Y. Kwon, K.-H. Kim, K.-B. Lee and J. S. Son, *Tissue Eng. Regener. Med.*, 2012, **9**, 175–183.
8 J. W. Lee, K. S. Kang, S. H. Lee, J.-Y. Kim, B.-K. Lee and D.-W. Cho, *Biomaterials*, 2011, **32**, 744–752.
9 A. Khademhosseini and R. Langer, *Nat. Protoc.*, 2016, **11**, 1775–1781.
10 R. Vishnubalaji, S. Yue, M. Alfayez, M. Kassem, F.-F. Liu, A. Aldahmash and N. M. Alajez, *Cancer Cell Int.*, 2016, **16**, 1–12.
11 N. Zhou, Q. Li, X. Lin, N. Hu, J.-Y. Liao, L.-B. Lin, C. Zhao, Z.-M. Hu, X. Liang and W. Xu, *Cell Tissue Res.*, 2016, **366**, 101–111.
12 N. Çakır-Özkan, S. Eğri, E. Bekar, B. Z. Altunkaynak, Y. B. Kabak and E. G. Kıvrak, *J. Oral Maxillofac. Surg.*, 2017, **75**, 221.e1–221.e14.
13 X. Zhao, Y. Han, J. Li, B. Cai, H. Gao, W. Feng, S. Li, J. Liu and D. Li, *Mater. Sci. Eng., C*, 2017, **78**, 658–666.
14 E. Tahmasebi, M. Alam, M. Yazdanian, H. Tebyanian and S. A. Mosaddad, *J. Mater. Res. Technol.*, 2020, **9**, 11731–11755.
15 H. Deutsch, *J. Spine*, 2010, **10**, e1–e4.
16 C. Ji, L. Bi, J. Li and J. Fan, *Int. J. Nanomed.*, 2019, **14**, 8271.
17 A. Rss, B. My, B. Et, C. Ay, B. Ht, B. Ak, D. Mrn and E. Yp, *Biocybern. Biomed. Eng.*, 2019, **39**, 789–796.
18 E. Mukwaya, F. Xu, M.-S. Wong and Y. Zhang, *Pharm. Biol.*, 2014, **52**, 1223–1228.
19 L. Wu, Z. Wei, S. He, Y. Bi, Y. Cao and W. Wang, *Curr. Drug Delivery*, 2021, **18**, 323–333.
20 X. Zhang, X. Lin, T. Liu, L. Deng, Y. Huang and Y. Liu, *Front. Pharmacol.*, 2019, **10**, 201.
21 C.-T. Che, M. S. Wong and C. W. K. Lam, *Molecules*, 2016, **21**, 239.
22 E. Shoba, R. Lakra, M. S. Kiran and P. S. Korrapati, *Mater. Sci. Eng., C*, 2018, **90**, 131–147.
23 J. Wang, X. Xiong and B. Feng, *Evid. Based Complement. Alternat. Med.*, 2013, **2013**, 1–16.
24 H. Wagner and G. Ulrich-Merzenich, *Evidence and Rational Based Research on Chinese Drugs*, Springer Science & Business Media, 2013.
25 S. Lin, L. Cui, G. Chen, J. Huang, Y. Yang, K. Zou, Y. Lai, X. Wang, L. Zou and T. Wu, *Biomaterials*, 2019, **196**, 109–121.

26 Y. Yuan and P. Zheng, *Research on Traditional Chinese Medicine*, 2002, pp. 53–54.
27 L. Cui, L. Y. Zhou, Y. Y. Liu, C. M. Ai, T. Wu and Y. Wu, *Chin. Pharmacol. Bull.*, 2004, **20**, 286–291.
28 X. He and Q. Shen, *BMC Complementary Altern. Med.*, 2014, **14**, 1–8.
29 Q. H. Huan and L. Cui, *Chin. Pharmacol. Bull.*, 2008, **24**, 978–979.
30 S. Lin, S. Qu, L. Chang, Y. Guo, K. Duan and J. Weng, *J. Wuhan Univ. Technol., Mater. Sci. Ed.*, 2013, **28**, 163–171.
31 L. Cui, T. Li, Y. Liu, L. Zhou, P. Li, B. Xu, L. Huang, Y. Chen, Y. Liu and X. Tian, *PLoS One*, 2012, **7**, e34647.
32 D. Xu, L. Xu, C. Zhou, W. Y. Lee, T. Wu, L. Cui and G. Li, *Int. J. Biochem. Cell Biol.*, 2014, **51**, 1–9.
33 B. Ghafoor, A. Aleem, M. N. Ali and M. Mir, *J. Drug Delivery Sci. Technol.*, 2018, **48**, 82–87.
34 R. Dorati, A. DeTrizio, T. Modena, B. Conti, F. Benazzo, G. Gastaldi and I. Genta, *Pharmaceuticals*, 2017, **10**, 96.
35 D. Khayatan, H. Tebyanian, A. Seifalian, K. Abbasi and M. Alam, *Evid. base Compl. Alternative Med.*, 2021, 9011226.
36 F. Fattahi, A. Khoddami and O. Avinc, *Nanomed. Res. J.*, 2019, **4**, 130–140.
37 Z. Yang, C. Sun, L. Wang, H. Chen, J. He and Y. Chen, *J. Colloid Interface Sci.*, 2017, **507**, 344–352.
38 S. Lappe, D. Mulac and K. Langer, *Int. J. Pharm.*, 2016, **517**, 338–347.
39 H. Zhao, R. Ding, X. Zhao, Y. Li, L. Qu, H. Pei, L. Yildirimer, Z. Wu and W. Zhang, *Drug Discovery Today*, 2017, **22**, 1302–1317.
40 S. Liu, Y. Zheng, Z. Wu, J. Hu and R. Liu, *Polymer*, 2020, **211**, 123093.
41 S. Q. Liu, R. L. Liu and R. Y. Rao, *Chin. J. Mater. Res.*, 2018, **32**, 913–920.
42 S. Liu, Y. Zheng, J. Hu, Z. Wu and H. Chen, *New J. Chem.*, 2020, **44**, 17382–17390.
43 S. Liu, X. Wu, J. Hu, Z. Wu and Y. Zheng, *New J. Chem.*, 2021, **45**, 10788–10797.
44 G. Yin, Y. Zhang, S. Wang, D. Shi, Z. Dong and W. Fu, *J. Biomed. Mater. Res. A*, 2010, **93**, 158–163.
45 S. Haghjooy Javanmard, J. Anari, A. Zargar Kharazi and E. Vatankhah, *J. Biomater. Appl.*, 2016, **31**, 438–449.
46 S. Alippilakkotte, S. Kumar and L. Sreejith, *Colloids Surf., A*, 2017, **529**, 771–782.
47 L. Gardella, M. Forouharshad, L. Pastorino and O. Monticelli, *Eur. Polym. J.*, 2017, **91**, 21–30.
48 E. Shoba, R. Lakra, M. S. Kiran and P. S. Korrapati, *Biomed. Mater.*, 2017, **12**, 035005.
49 T. Xu, Q. Yao, J. M. Miszuk, H. J. Sanyour, Z. Hong, H. Sun and H. Fong, *Colloids Surf., B*, 2018, **171**, 31–39.
50 X. Wang, G. Song and T. Lou, *J. Mater. Sci.: Mater. Med.*, 2010, **21**, 183–188.
51 L. Liu, J. Li, Y. Zhang, S. Zhang, J. Ye, Z. Wen, J. Ding, S. P. Kunapuli, X. Luo and Z. Ding, *Thromb. Res.*, 2014, **134**, 866–876.
52 Z. Ren, X. Wang, S. Wang, C. Zhai, Y. He, Y. Zhang and Y. Qiao, *Bio-Med. Mater. Eng.*, 2014, **24**, 1333–1340.
53 C. Ma, Y. Yao, Q.-X. Yue, X.-W. Zhou, P.-Y. Yang, W.-Y. Wu, S.-H. Guan, B.-H. Jiang, M. Yang and X. Liu, *PLoS One*, 2011, **6**, e14692.
54 J. O. Orgah, S. He, Y. Wang, M. Jiang, Y. Wang, E. A. Orgah, Y. Duan, B. Zhao, B. Zhang and J. Han, *Pharmacol. Res.*, 2020, **153**, 104654.
55 L. Ren, S. Pan, H. Li, Y. Li, L. He, S. Zhang, J. Che and Y. Niu, *Sci. Rep.*, 2018, **8**, 1–13.